

# Improved dynamic model of a bulb turbine-generator for analysing oscillations caused by mechanical torque disturbance on a runner blade

Miljenko Brezovec<sup>a,\*</sup>, Igor Kuzle<sup>b</sup>, Matej Krpan<sup>b</sup>, Ninoslav Holjevac<sup>b</sup>

<sup>a</sup> HEP-Proizvodnja d.o.o., 42000 Varazdin, Croatia

<sup>b</sup> University of Zagreb, Faculty of Electrical Engineering and Computing, 10000 Zagreb, Croatia

## ARTICLE INFO

### Keywords:

Electromechanical oscillations  
Natural frequency  
Mathematical model  
Hydroelectric unit  
Bulb turbine

## ABSTRACT

Generic dynamic models of hydraulic turbines are unable to capture power oscillations phenomena originating from a torque disturbance on a single runner blade. In this paper, an improved dynamic model of a double-regulated hydraulic turbine which takes into account torque oscillations identified from draft tube pressure measurements was presented. It was experimentally identified that specific power oscillations of a bulb turbine operating with low tailwater level can be connected to cavitation-related phenomena on a single runner blade. Furthermore, it was shown that these oscillations do not originate from grid fault-induced resonance between the turbine rotor and generator, nor from the excitation system. The proposed simulation model was validated against measurement data of hydro power plant Dubrava and the validation shows good agreement between measured and simulated results.

## 1. Introduction

There are many sources of power system oscillations as described in [1,2] while power swings in hydroelectric power plants (HPPs) have been analyzed since 1930s [3]. Beside power swings, many different types of vibrations and oscillations appear in operation of turbine-generator units in hydroelectric power plants, with different causes and consequences [4–6]. Forced oscillations of hydraulic turbine-generators originate from periodical disturbances of the mechanical torque caused by different flow-induced phenomena [7–9]:

- low-frequency oscillations are usually related to draft tube vortex which is characteristic for Francis turbines;
- oscillations on runner frequency can be caused by unbalance of turbine runner, asymmetry of casing or cavitation-related phenomena;
- high frequency phenomena are usually related to turbine rotor-stator interaction.

Hydro turbine-generator is an extremely complex, multivariate nonlinear dynamic system consisting of hydraulic, mechanical and electrical subsystems which requires a detailed mathematical model to adequately describe its behavior. The level of detail of the mathematical model depends on the type of phenomena being studied. Basic elements of a hydroelectric turbine-governor are the hydraulic turbine

with penstock and tunnel dynamics, turbine governor and a generator.

Modelling and analysis of hydroelectric power plant dynamics has been a subject of many studies throughout many decades, therefore this area is already well-researched and there is very little to none novel research on dynamic modelling for power system stability studies. Detailed modelling of synchronous generators and impact of excitation systems on electromechanical oscillations can be found in [10,11], respectively. Detailed modelling of hydraulic turbines and hydraulic turbine governing systems can be found in [12–17].

In [18], authors present a nonlinear hydro turbine model for studying hydraulic transients induced by large load rejections. Unified dynamic model of Francis turbine incorporating unbalanced forces on the turbine runner was presented in [19]. It unifies the interaction between the electrical, mechanical and hydraulic subsystems for analyzing dynamic coupling between different states of the system. Zhang et al. [20] studied the dynamic evolution of the turbine-governing system of a hydro plant under periodic excitation. In [21], very low frequency oscillations were studied; the oscillations appear in the grid caused by the instability of the hydro turbine governing system of a large hydroelectric power plant asynchronously connected to the grid via HVDC lines. Other works [22–24] also studied low-frequency oscillations in the power grid.

Because of their construction and horizontal arrangement, there are different causes of pulsations and vibrations in bulb turbines. The entire unit is usually fixed by upper and lower stays, and lateral supports.

\* Corresponding author.

E-mail addresses: [miljenko.brezovec@hep.hr](mailto:miljenko.brezovec@hep.hr) (M. Brezovec), [igor.kuzle@fer.hr](mailto:igor.kuzle@fer.hr) (I. Kuzle), [matej.krpan@fer.hr](mailto:matej.krpan@fer.hr) (M. Krpan), [ninoslav.holjevac@fer.hr](mailto:ninoslav.holjevac@fer.hr) (N. Holjevac).

**Nomenclature**

$\Delta$	Small deviation of a variable around its initial operating point
$\delta$	$q$ -axis phase shift with respect to reference axis; Load angle
$\cdot$	Time derivative
$\eta_t$	Turbine efficiency
$\omega$	Angular frequency
$\Psi_d, \Psi_q$	Stator winding $d$ and $q$ axis flux linkage
0	Subscript denoting initial (steady-state) value
$d, D$	Subscript denoting $d$ -axis value
$q, Q$	Subscript denoting $q$ -axis value
$D$	Turbine-generator damping constant
$H$	Turbine-generator inertia constant
$h$	Turbine head
$i_d, i_q$	Generator $d$ and $q$ axis current
$i_F, i_D, i_Q$	Field winding current, damper winding $d$ and $q$ axis current
$i_{abc}$	Generator instantaneous three-phase current

$k$	Mutual inductance coefficient
$L_d, L_q$	$d$ and $q$ axis stator winding inductance
$L_F, L_D, L_Q$	Field winding inductance, damper winding $d$ and $q$ axis inductance
$M_F, M_D, M_Q$	Armature winding and field winding mutual inductance, damper winding $d$ and $q$ axis mutual inductance
$M_m$	Mechanical torque
$p_{dt}$	Draft tube pressure
$q$	Turbine flow
$r$	Armature winding resistance
$r_F, r_D, r_Q$	Field winding resistance, damper winding $d$ and $q$ axis resistance
$T_o$	Oscillating torque due to runner blade disturbance
$T_t$	Turbine torque due to head, flow and turbine governor
$T_W$	Water starting time
$v_d, v_q$	Generator $d$ and $q$ axis terminal voltage
$v_F, v_D, v_Q$	Field winding voltage, damper winding $d$ and $q$ axis voltage
$v_{abc}$	Generator instantaneous three-phase terminal voltage
$y_W, y_R$	Guide vane opening; Rotor blade angle

Hence, axial asymmetry of inner flow field can occur. Because of the horizontal position and the large runner diameter, the gravity has a significant influence on the internal flow of the turbine. There is a vertical pressure gradient caused by the gravity which must be taken into account in the analysis [25]. The pressure above the free surface is the constant atmospheric pressure, and the pressure increases with the water depth which results in hydraulic flow imbalance. The inhomogeneous pressure distribution results in a pressure variation along the blades during rotation. If conditions for cavitation exist, due to the difference in hydrostatic pressure on runner blades cavitation on the blade in the upper position is much more intensive than cavitation on the blade in the bottom position [26,27]. During rotation, cavitation intensity at each blade increases when the blade rotates up and decreases when it rotates down. The asymmetric locality and periodicity of cavitation occurrence lead to the hydraulic imbalance and oscillation.

### 1.1. Problem formulation

The main motivation behind this paper are the power oscillation phenomena of the turbine-generator in HPP Dubrava in Croatia with basic turbine information given in Table 1. Power oscillations have been present since the first commissioning of the hydropower plant in 1989.

In normal, undisturbed operation, power oscillations are negligible in all operating conditions, while disturbances which result in an increased power oscillations appear occasionally on both machines [28,29]. Amplitudes of these oscillations depend on the active power set-point and reach their maximum near the rated power operation. Frequency of these oscillations corresponds to the rotor speed regardless of the operating conditions. Several different research studies on the HPP Dubrava power oscillations were carried out and two main theories have been discussed:

1) First approach to the explanation of these phenomena is that the units loaded near maximum power enter resonance mode. Natural frequency of electromechanical oscillations depends on the working conditions and can be close to the rotor speed frequency [30]. In such conditions, disturbance of mechanical torque produces power oscillations which can be significantly amplified due to the electromechanical resonance.

2) Second approach starts from the mechanical torque as the main cause of oscillations because for the same operating conditions power oscillations are negligible until a step disturbance occurs. There are indications that mechanical torque disturbances relate to the turbine

cavitation [31].

It should be emphasized that the plant operates with the tailwater level lower than it was designed for [32] which increases the cavitation risk. Probability of increased power oscillations is bigger if the second unit is not in operation, especially during trash rack cleaning. This indicates that a mechanical torque disturbance could be a trigger for such behavior. Peak-to-peak values of power oscillations are usually up to 3% of nominal power, but few cases with 10% or more have also been recorded. To decrease big power oscillations when they appear, the power of the unit should be lowered and, in most cases, the only solution to eliminate them is stopping the unit [29]. Such cases appear occasionally, but each unit is being stopped for more than 10 times a year because of this behavior.

### 1.2. Contribution

Power swings and oscillations can be a frequent operating problems in some HPP units. Most of the surveyed literature on these phenomena deals with Francis turbines since they are the most used and also characterized by flow-induced power swings in the rough zone. Considerably less examples can be found on units with Kaplan turbines and particularly specific are units with horizontal bulb turbines. Moreover, the surveyed literature mostly studied low-frequency oscillations in the power grid or the impact of turbine-governing on the power oscillations of the hydro power system. We found that none of the known generic models can be used to simulate the type of oscillations that can appear in bulb turbines operating with low tailwater level, e.g. HPP Dubrava. These generic hydro turbine models are suitable for governing studies, transient stability studies and long-term dynamics studies which are not the issues related to the problems in HPP Dubrava. Although different cases of hydro unit power oscillations can be found in literature, no literature was found that investigated hydro turbine oscillations on rotor frequency appearing randomly during normal operation in steady-state. These oscillations result in

**Table 1**  
Basic information about HPP Dubrava turbine.

Rated power	$2 \times 39$ MW
Turbine type	Bulb
Runner diameter	5.5 m
Synchronous speed	125 rpm
Rated flow	250 m <sup>3</sup> /s
Turbine head	16–20 m

reduced average power and the power plant must be stopped which results in the loss of revenue for the plant operator and increased fatigue of the hydraulic system. Moreover, these oscillations are transferred to the grid and reduce the power quality at the point of connection.

Therefore, the main contributions of this paper are as follows:

- procedure for identification of the single runner blade disturbance as the source of power oscillations;
- improved dynamic model of a bulb hydraulic turbine for studying power oscillations originating from a periodical torque disturbance on a runner blade;
- validation of the proposed model using measurements from a real hydroelectric unit (HPP Dubrava);
- practical experience in the research of electromechanical oscillations of bulb turbines.

## 2. Identification and elimination of the cause of disturbance

Measurements of the power oscillations in HPP Dubrava have been recorded throughout the years using specialized monitoring systems. Initially, many possible causes for power oscillations were regarded, such as electromechanical resonance between the generator and the rotor, grid-side disturbance (e.g. fault in the transmission network) or issues in the power system stabilizer or excitation circuits. It will be shown in this section that all but one cause have been eliminated and the actual cause of disturbance has been narrowed down to a disturbance on a single runner blade as most probable.

Fig. 1 shows typical waveform of the power oscillations recorded at rated operating point. The power oscillations appear during normal steady-state operation near rated power. It can be seen that the power oscillations (red curve) result in the reduction of average power (blue curve) although the turbine flow and opening remain unchanged. Otherwise, change in gate opening and consequently the water flow would result in the change of output power.

### 2.1. Transmission network disturbance

Disturbance in the transmission network (Fig. 2) has been ruled out as the possible cause of disturbance due to the fact that the dominant frequency of electromechanical oscillations of the generator during a disturbance is significantly bigger than the rotor speed frequency and corresponds to the natural frequency of the system which is shown in Fig. 3 (identified from measurements to be around 2.7 Hz). Rotor frequency is 2.0833 Hz (because the speed is 125 rpm as noted in Table 1) while the natural frequency is around 2.7 Hz (theoretically, at nominal

operating point). Natural frequency was calculated using standard modal analysis of a linearized 7th order synchronous generator model described by (1)–(3) [10], in which all the variables and parameters are defined in the Nomenclature at the beginning of the paper. State-space model (1) is of the form  $\dot{\mathbf{v}} = -\mathbf{K}\mathbf{x} - \mathbf{M}\dot{\mathbf{x}}$  which can be easily converted to the classical form  $\ddot{\mathbf{x}} = \mathbf{A}\mathbf{x} + \mathbf{B}\dot{\mathbf{x}}$  by transformations  $\mathbf{A} = -\mathbf{M}^{-1}\mathbf{K}$  and  $\mathbf{B} = -\mathbf{M}^{-1}$ . Eigenvalues of  $\mathbf{A}$  determine the stability of the linear system.

$$\begin{bmatrix} \Delta v_d \\ -\Delta v_F \\ 0 \\ \Delta v_q \\ 0 \\ \Delta T_m \\ 0 \end{bmatrix} = -\mathbf{K} \begin{bmatrix} \Delta i_d \\ \Delta i_F \\ \Delta i_D \\ \Delta i_q \\ \Delta i_Q \\ \Delta \omega \\ \Delta \delta \end{bmatrix} - \mathbf{M} \begin{bmatrix} \Delta \dot{i}_d \\ \Delta \dot{i}_F \\ \Delta \dot{i}_D \\ \Delta \dot{i}_q \\ \Delta \dot{i}_Q n \\ \Delta \dot{\omega} \\ \Delta \dot{\delta} \end{bmatrix} \quad (1)$$

$$\mathbf{K} = \begin{bmatrix} r & 0 & 0 & \omega_0 L_q & \omega_0 kM_Q & \Psi_{q0} & 0 \\ 0 & r_F & 0 & 0 & 0 & 0 & 0 \\ 0 & 0 & r_D & 0 & 0 & 0 & 0 \\ -\omega_0 L_d & -\omega_0 kM_F & \omega_0 kM_D & r & 0 & 0 & 0 \\ 0 & 0 & 0 & 0 & r_Q & 0 & 0 \\ \frac{\Psi_{q0} - L_d i_{q0}}{3} & \frac{-kM_F i_{q0}}{3} & \frac{-kM_D i_{q0}}{3} & \frac{-\Psi_{d0} + L_q i_{d0}}{3} & \frac{-kM_Q i_{d0}}{3} & -D & 0 \\ 0 & 0 & 0 & 0 & 0 & -1 & 0 \end{bmatrix} \quad (2)$$

$$\mathbf{M} = \begin{bmatrix} L_d & kM_F & kM_D & 0 & 0 & 0 & 0 \\ kM_F & L_F & M_R & 0 & 0 & 0 & 0 \\ kM_D & M_R & L_D & 0 & 0 & 0 & 0 \\ 0 & 0 & 0 & L_q & kM_Q & 0 & 0 \\ 0 & 0 & 0 & kM_Q & L_Q & 0 & 0 \\ 0 & 0 & 0 & 0 & 0 & -2H & 0 \\ 0 & 0 & 0 & 0 & 0 & -1 & 1 \end{bmatrix} \quad (3)$$

Results correspond to the expected value defined by the turbine manufacturer as well as the measurements. Since modal analysis is a standard procedure for determining the characteristics of a linearized dynamic system, it will not be described here. Methodology from [10] was used and for the actual calculation procedure we refer the reader to [33].

Natural frequency of the system depends on its initial conditions, active and reactive power, that is shown in Fig. 4. Fig. 4 shows that the natural frequency is significantly different than the rotor frequency (depicted with black line  $\omega_0$ ) for all normal operating points. The only region where both the rotor frequency and the natural frequency are same or similar and where resonance may occur is when the generator

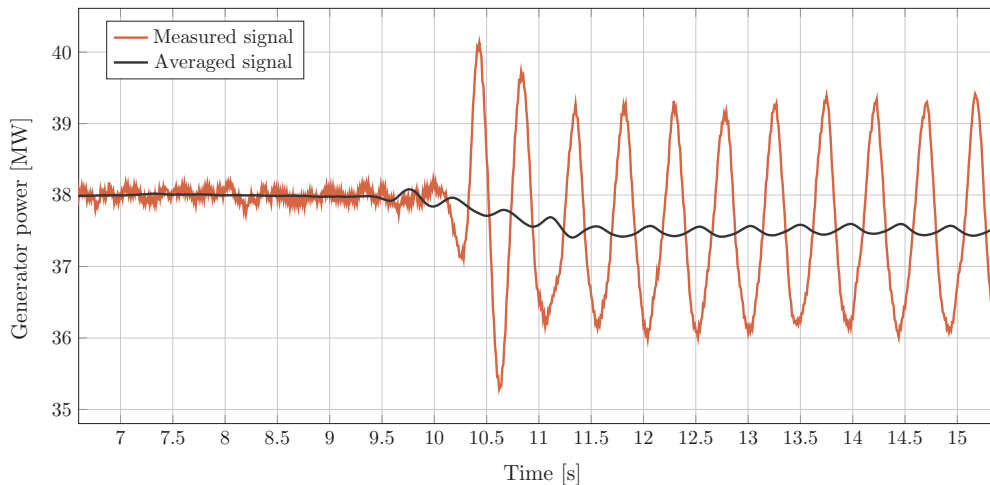


Fig. 1. Power oscillations in HPP Dubrava during normal operation.

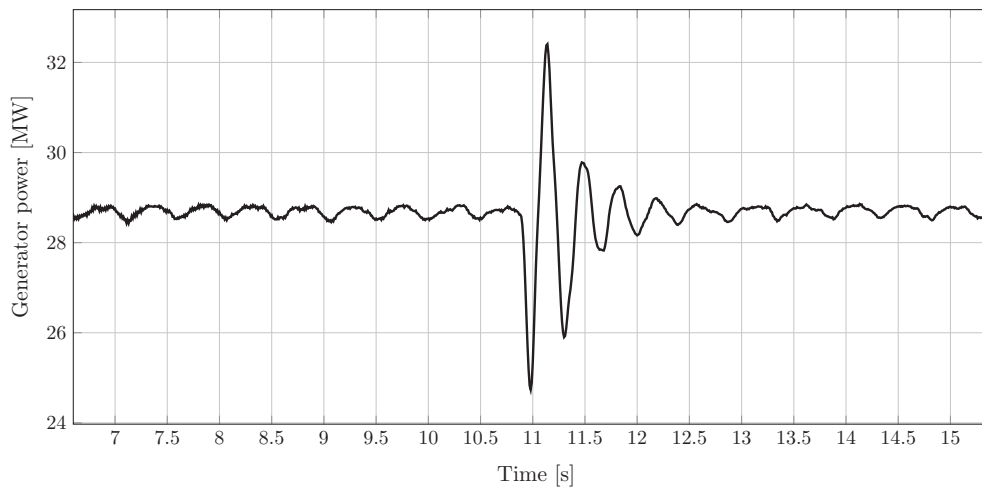


Fig. 2. HPP Dubrava power oscillations during a transmission network disturbance.

operates at very low active power output and consumes reactive power. However, the plant never operates in this region; it operates at rated power and works with either unity power factor or produces reactive power. Therefore, the electromechanical resonance between the turbine and the generator is disregarded as the source of oscillations.

2.2. Excitation system and power system stabilizer

Fig. 5 shows the measurements of the electrical quantities during reported oscillations (non-fault related). With PSS (power system stabilizer) actions, the oscillations are partially transferred from active power signal to the voltage control signals (generator terminal voltage and reactive power). This is visible in Fig. 5 which shows an example of power oscillations appearance with active PSS (control function switches off the PSS 10 s after oscillations begin at  $t = 0$  s). In other words, in the presence of forced oscillations active power oscillations can be partially reduced by PSS action on the expense of increased reactive power oscillations. Switching to manual excitation also did not resolve the oscillations. Therefore, because the oscillations persisted regardless of whether the PSS is switched on or off, the effects of PSS and AVR (automated voltage regulation) were also disregarded as the possible source of oscillations.

2.3. Runner blade disturbance

To identify the phenomena in water flowing through the turbine,

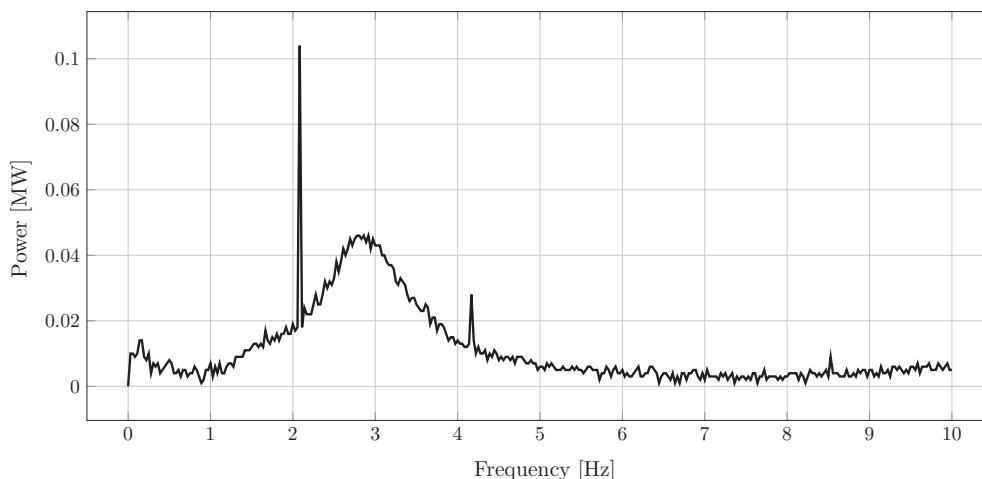


Fig. 3. Spectral analysis of the HPP Dubrava power oscillation during transmission network disturbance.

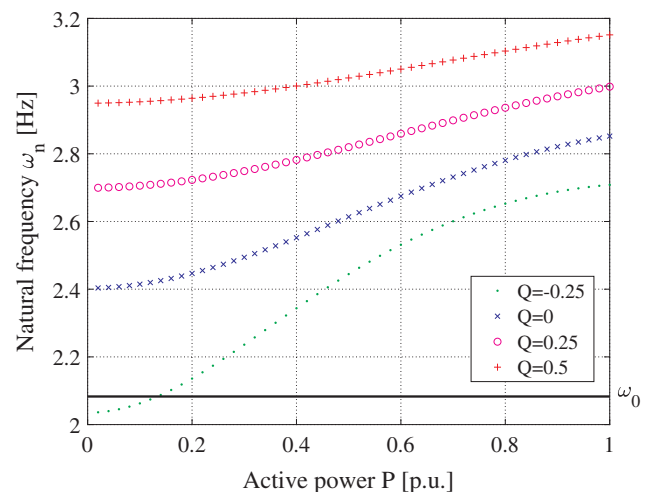


Fig. 4. Generator natural frequency as a function of active and reactive power loading.

continuous measurement of pressure pulsations in draft tube was implemented. In normal conditions, pressure pulsates in regular rhythm of 4 times per turn, which corresponds to the passing of the 4 runner blades. When disturbance appears, uniform pulsation rhythm of 4 times per turn is changed and additional component appears with a frequency

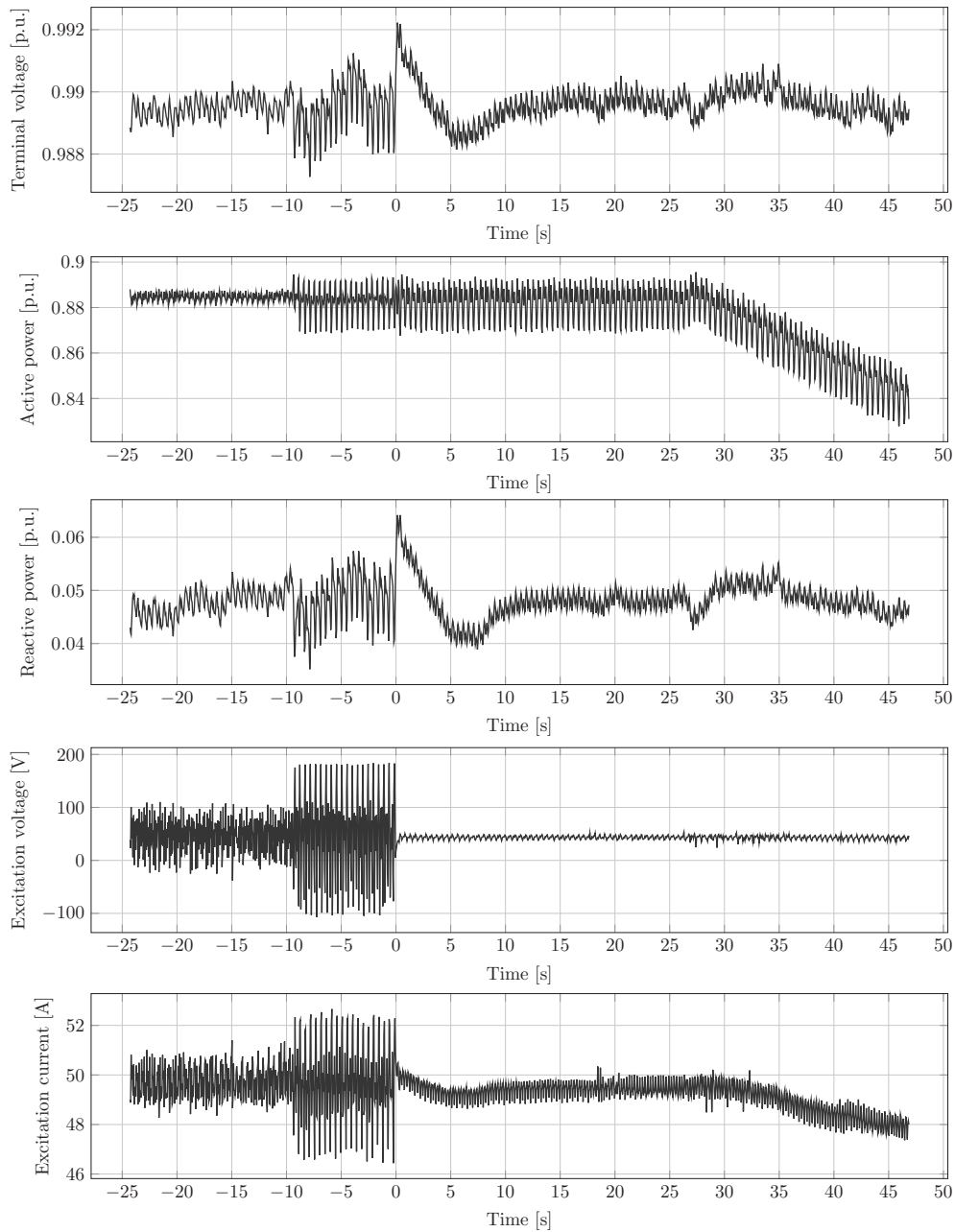


Fig. 5. Measured electrical quantities during oscillations—top to bottom: terminal voltage, active power, reactive power, excitation voltage, excitation current.

of once per turn (Fig. 6). This component can be identified by averaging the signal over  $1/4$  of the rotor turn. The mechanical torque which serves as an input to the generator model is identified from these waveforms. The waveform of pressure pulsations during the disturbance significantly deviates from the normal, pre-disturbance waveform while the exact waveform also depends on the operating point. Nevertheless, for all operating points, the frequency of the first harmonic of the pressure pulsations is disturbed which distorts the pre-disturbance waveform with dominant fourth harmonic. This distortion may vary and the increase in draft tube pressure in every cycle causes short-term reduction of the mechanical torque.

In all cases, power oscillations' frequency is equal to rotor speed frequency with dominant first harmonic. Initially, oscillations were considered to have a sinusoidal form. Analysis of many waveform records has shown that waveforms deviate from assumed sinusoidal form depending strongly on the operating point. Although there are many

different waveforms, basic samples are repeated in most cases. Regardless of the waveform, first harmonic (2.083 Hz) remains dominant. Analysis of characteristic cases showed that the phase shift of power oscillations' first harmonic is approximately equal to one of four discrete values (Fig. 7) which correspond to one of the four runner blades.

This leads to a very important conclusion: every appearance of power oscillations can be correlated to a disturbance on a specific runner blade. In this regard, the assumption about disturbed flow on one runner blade and cavitation-connected phenomena whose intensity is changing with rotation of the blade becomes completely realistic. Although only results for unit A are shown, the same behavior was recorded for both units during many occurrences of oscillations.

Since such a disturbance is characterized by an extra component which pulsates inside one complete turn of the runner, this behavior cannot be captured by the generic turbine-governor model due to much

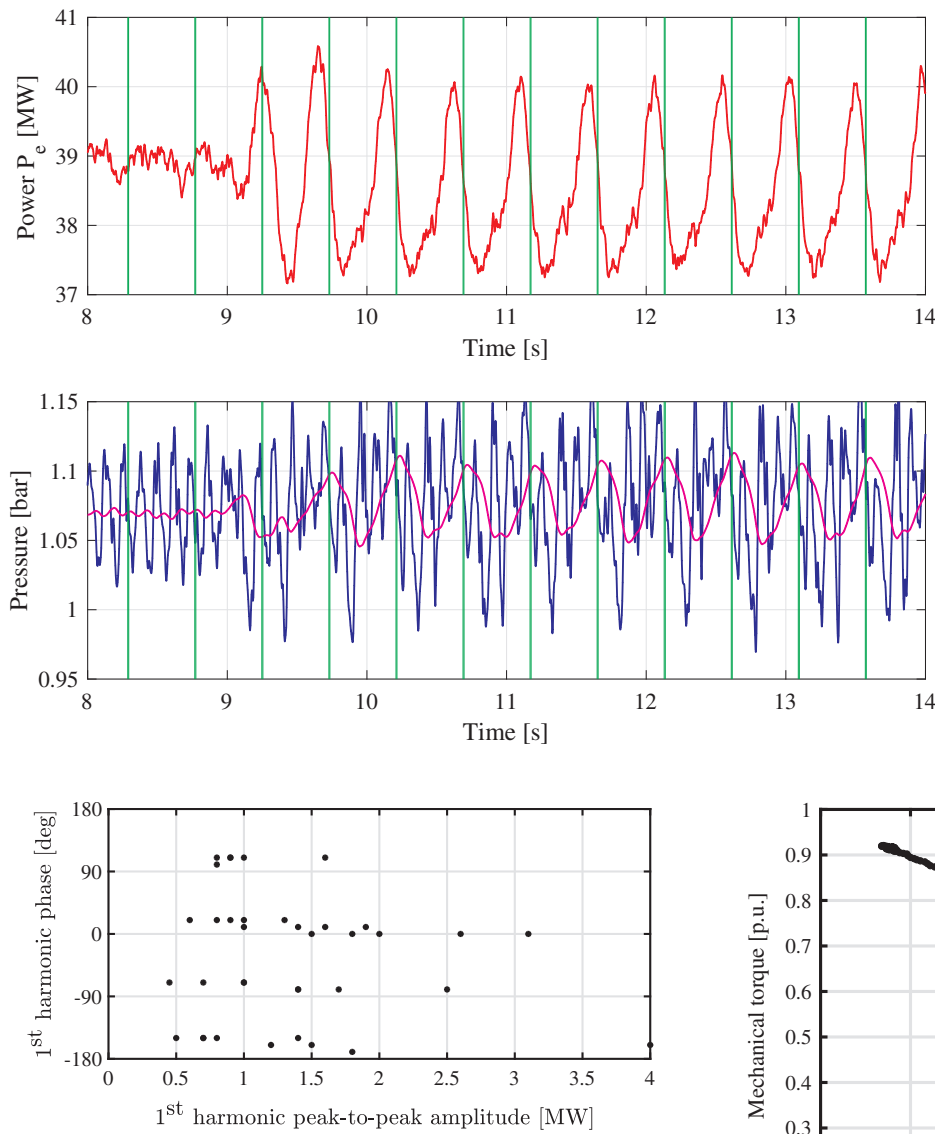


Fig. 7. Phase of the first harmonic of oscillations (unit A)-4 discrete value regions correspond to 4 runner blades.

Fig. 6. Active power and draft tube pressure pulsations—top: active power; bottom: draft tube pressure (blue), draft tube pressure averaged signal (magenta). Green markers mark one complete turn of the runner. (For interpretation of the references to color in this figure legend, the reader is referred to the web version of this article.)

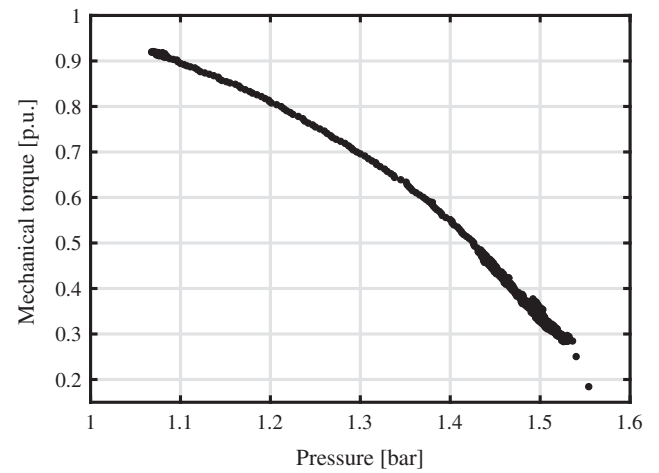


Fig. 9. Mechanical torque vs. draft tube pressure in steady-state condition.

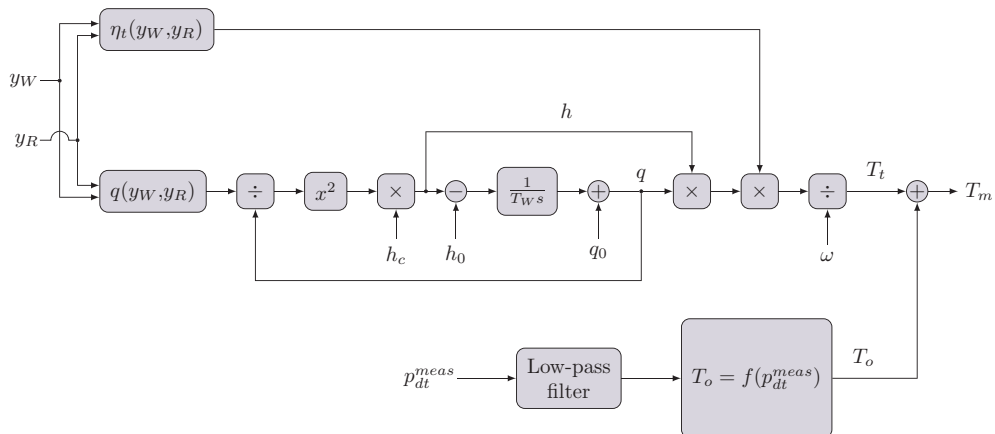
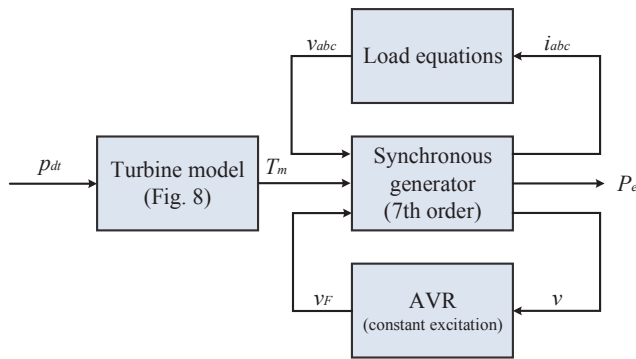


Fig. 8. Proposed nonlinear model of a double-regulated bulb turbine including periodic torque disturbance.

**Table 2**  
HPP Dubrava synchronous generator parameters.

Parameter	Symbol	Value
Nominal power	$S_n$	42 MVA
Nominal voltage	$U_n$	6.3 kV
frequency	$f_n$	50 Hz
$d$ -axis synchronous reactance	$X_d$	1.346 p.u.
$d$ -axis transient reactance	$X'_d$	0.446 p.u.
$d$ -axis subtransient reactance	$X''_d$	0.330 p.u.
$q$ -axis synchronous reactance	$X_q$	0.940 p.u.
$q$ -axis subtransient reactance	$X''_q$	0.371 p.u.
Armature leakage reactance	$X_l$	0.243 p.u.
$d$ -axis transient time constant	$T'_d$	0.550 s
$d$ -axis subtransient time constant	$T''_d$	0.029 s
$q$ -axis subtransient time constant	$T''_q$	0.029 s
Armature winding resistance	$R_a$	0.006 $\Omega$
Inertia constant	$H$	0.9 s



**Fig. 10.** Turbine-generator system used in simulations.

larger time constants. This has given the motivation to expand the generic model with an additional oscillating torque component identified from draft tube pressure measurements as described in Section 3.

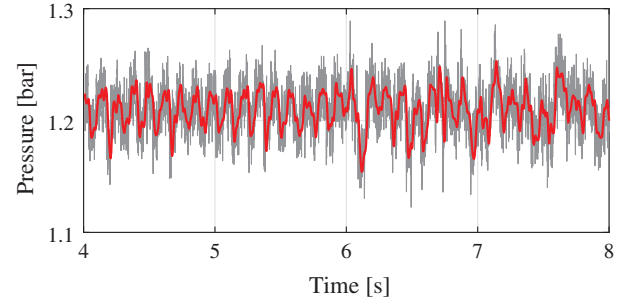
### 3. Description of the proposed model

The proposed model is shown in Fig. 8. It consists of two parts: the upper part is a standard dynamic model of a double-regulated bulb turbine from [15] which outputs the turbine torque  $T_t$ . This model is expanded with the bottom part which outputs the oscillating torque  $T_o$  estimated from the draft tube pressure measurement  $p_{dt}^{meas}$ . Total mechanical torque  $T_m$  is then equal to  $T_t + T_o$ . The rest of the variables are as follows:  $h$ ,  $q$  are turbine head and turbine flow, respectively;  $h_0$ ,  $q_0$  are the static head and initial flow, respectively;  $h_c$  is the characteristic head for which the turbine characteristics are defined.  $q(y_W, y_R)$  and  $\eta_t(y_W, y_R)$  are the functions of the flow and turbine efficiency with respect to variables  $y_W$  and  $y_R$ . These functions are experimentally defined for a given turbine.  $y_W$  is the position of the stator blades servo piston corresponding to the opening of the guide vane, while  $y_R$  is the position of the rotor blades servo piston corresponding to the rotor blade angle.  $y_W$  and  $y_R$  are the outputs of turbine-governor. All variables and constants are in p.u. Mathematical model of the double-regulated bulb hydro turbine is described by (4)–(6), where  $T_W$  is the water starting time.

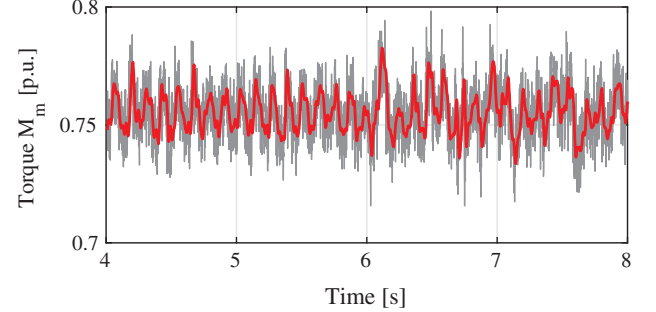
$$\frac{d(q - q_0)}{dt} = -\frac{1}{T_W}(h - h_0) \quad (4)$$

$$q = q(y_W, y_R) \sqrt{\frac{h}{h_c}} \quad (5)$$

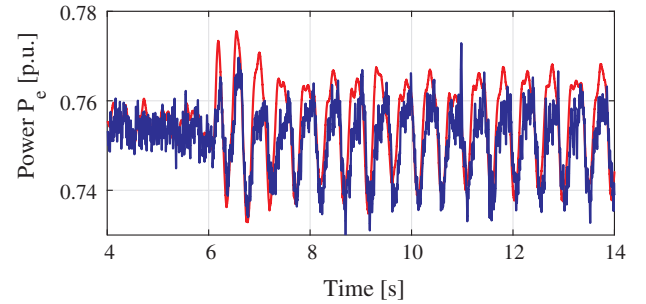
$$T_t = \frac{q \cdot h \cdot \eta_t(y_W, y_R)}{\omega} \quad (6)$$



(a) Unit A draft tube pressure: measurement (gray), filtered signal (red)



(b) Unit A mechanical torque: base signal (gray), filtered signal (red)



(c) Unit A generator power: measurement (blue), simulation (red)

**Fig. 11.** Results of model validation on unit A.

The turbine torque model ( $T_t$ ) cannot be used to describe the oscillations caused by the torque disturbance on a single runner blade for two reasons:

1. it lacks the proper input for the source of the oscillating component—the turbine torque is only a function of turbine speed  $\omega$  and the control actions from the turbine governor  $y_W$  and  $y_R$ .
2. The time constant of the turbine torque dynamics is equal to the water starting time  $T_W$  whose order of magnitude is around 1 s. On the other hand, disturbances on a single runner blade have a much smaller time constant since this is something that happens inside one complete turn of the turbine rotor.

Relationship between the mechanical torque and the draft tube pressure can be experimentally identified from draft tube pressure measurements in steady-state. Such a curve is shown in Fig. 9. Subtracting the average value of the torque from the total mechanical torque (identified from draft tube pressure), the oscillating torque can be extracted since the average torque should be equal to the torque at power set-point because the turbine should be operating at constant power and synchronous speed, but is oscillating around that value instead.

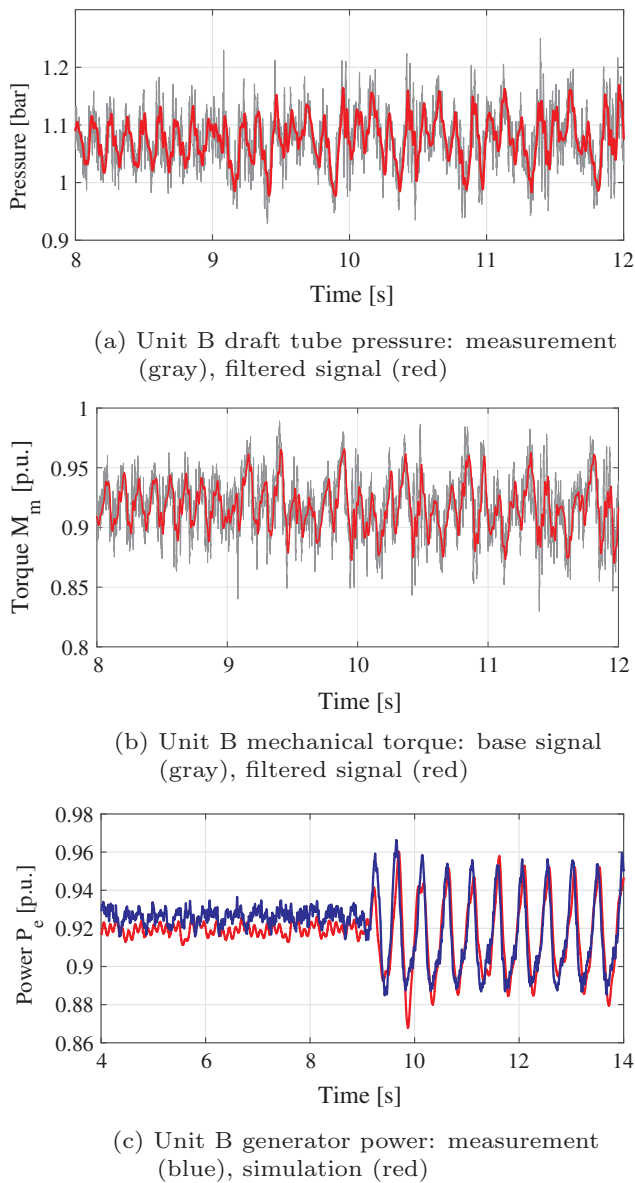


Fig. 12. Results of model validation on unit B.

**Table 3**  
Accuracy of the proposed model.

Type of error	Unit A	Unit B
Maximum absolute error	0.02 p.u.	0.03 p.u.
Maximum relative error	2.91%	-3.34%
Root mean square error	0.69%	0.97%

#### 4. Experimental validation of the model

Proposed simulation model from Fig. 8 is experimentally validated using measured data from HPP Dubrava for both units. Synchronous generator parameters of HPP Dubrava are given in Table 2. Constant excitation was used since it was shown that the excitation system does not have an impact on the oscillations. Due to the characteristics of the observed phenomena and the time domain in which they are analyzed, the key element of the model is the synchronous generator which is modeled in detail as a 7th order model. The complete system is shown in Fig. 10. The input of the system is the draft tube pressure used to identify the mechanical torque of the turbine. The output of the system

is the active power of the generator. Simulations are shown for two instances of oscillations appearance: unit A on April 11th, 2018 and unit B on May 25th, 2018. Simulations are conducted in MATLAB-Simulink software package.

Figs. 11a and 12a show the draft tube pressure measurement for units A and unit B, respectively. To identify the mechanical torque the original signal was used, but these figures also show the filtered signal where the difference between the regular pulsations (4 times per turn) and irregular pulsations is more visible; Figs. 11b and 12b show the mechanical torque identified from the pressure measurements  $T_m = f(p_{dt})$ . A sample of pressure pulsations both before and after disturbance is used. Analysis of power oscillations shows good agreement between measured and simulated results (Figs. 11c and 12c). The analysis of error between simulated and measured results (shown in Table 3) for output power (Figs. 11c and 12c) confirm that the model accurately describes the actual plant. Of course, the simulated results do not perfectly correspond to the measured results due to the following reasons:

- The model can only so accurately represent an actual complex system with many nonlinearities which are not captured by the model, especially in the case when many electrical, hydraulic and mechanical subsystems are interconnected;
- Measured data contains noise and measurement error that impact the simulation results. Moreover, measurement data is filtered so there is some additional loss of data.

Nevertheless, the simulation model adequately captures the general dynamic behavior of a large bulb turbine for a runner blade disturbance. This model can be used to predict the impact of oscillations on the hydraulic system fatigue and to develop different solutions for the reduction or removal of these oscillations.

#### 5. Conclusion

In this paper, we have developed a model for the analysis of power oscillations originating from a bulb turbine torque disturbance caused by an efficiency decrease of a single runner blade. It was shown that generic hydraulic turbine models cannot capture disturbance phenomena on the runner blade inter-turn time scale.

By using experimental data and modal analysis, we have shown that this specific power oscillations phenomenon does not originate from turbine-generator electromechanical resonance caused by a grid-side disturbance nor from the effects of the power system stabilizer and excitation system. On the other hand, it was shown that based on the phase shift of the dominant harmonic of the power oscillations the power oscillations can be correlated to a disturbance on a specific runner blade.

The proposed model is validated using real measurement data on both units in HPP Dubrava and experimental validation has shown that the simulated and measured results show very good alignment with relative error of less than 3.5%. The proposed model can be easily integrated with generic hydro turbine models found in many power system simulation software packages. The main drawback is that draft tube pressure measurements must be available if an exact disturbance is to be simulated. Nevertheless, for generic simulations it is enough to manually generate the oscillating torque waveform as described in this paper. Thus, different oscillating torque components can be generated and applied to study the impact on electromechanical oscillations.

Power oscillations caused by disturbances on the runner blade increase the wear and tear of the hydraulic equipment, reduce the power quality and the decrease the revenue of the power plant. The proposed model can be used to study the impact of these oscillations on power quality as well as for developing procedures aimed to reduce or eliminate these oscillations. The importance of these findings lies in the ability to model these oscillations during the design stage of the bulb

turbines. Further research will include additional improvement of the presented model to take into account the impact of the disturbance on the decrease of turbine efficiency; development of the numerical model of oscillating torque component as well as developing oscillating torque signal generator for generic studies.

### Declaration of Competing Interest

The authors declare that they have no known competing financial interests or personal relationships that could have appeared to influence the work reported in this paper.

### Acknowledgements

This work was supported by the European Structural and Investment Funds under project Konpro 2, grant KK.01.2.1.01.0096 and by the Croatian Science Foundation, Croatian Transmission System Operator (HOPS) and HEP Generation under the project WINDLIPS grant no. PAR-02-2017-03.

### References

- Ghorbaniparvar M. Survey on forced oscillations in power system. *J Modern Power Syst Clean Energy* 2017;5(5):671–82. <https://doi.org/10.1007/s40565-017-0273-4>.
- Ghorbaniparvar F, Sangrody H. Pmu application for locating the source of forced oscillations in smart grids. *IEEE power and energy conference at Illinois (PECI)* 2018. p. 1–5. <https://doi.org/10.1109/PECI.2018.8334996>.
- Rheingans W. Power swings in hydroelectric power plants. *Trans ASME* 1940;62(3):171–84.
- Wu Y, Li S, Liu S, Dou HS, Qian Z. *Vibration of hydraulic machinery*. Springer; 2013.
- Huynh D. *Vibration characteristics of hydro plant equipment*. Vibration Institute 24th annual meeting. 2000. p. 189–98.
- Jansson I. *The effect of flowing water on turbine rotor vibrations [Licentiate thesis]*. Luleå University of Technology; 2010.
- Dörfler P, Sick M, Couto A. *Flow-induced pulsation and vibration in hydroelectric machinery*. Springer; 2013.
- Mohanta RK, Chelliah TR, Allamsetty S, Akula A, Ghosh R. Sources of vibration and their treatment in hydro power stations-a review. *Eng Sci Technol Int J* 2017;20(2):637–48. <https://doi.org/10.1016/j.jestch.2016.11.004>. URL: <http://www.sciencedirect.com/science/article/pii/S2215098616304815>.
- Ohashi H. *Vibration and oscillation of hydraulic machinery*. CRC Press; 2016.
- Anderson PM, Fouad AA. *Power system control and stability*. 2nd ed. John Wiley & Sons; 2003.
- IEEE recommended practice for excitation system models for power system stability studies. *IEEE Std 421.5-2016 (Revision of IEEE Std 421.5-2005)*; 2016. p. 1–207. doi: 10.1109/IEEESTD.2016.7553421.
- Hydraulic turbine and turbine control models for system dynamic studies. *IEEE Trans Power Syst* 1992;7(1):167–79. doi: 10.1109/59.141700.
- De Jaeger E, Janssens N, Malfliet B, Van De Meulebroeke F. Hydro turbine model for system dynamic studies. *IEEE Trans Power Syst* 1994;9(4):1709–15. <https://doi.org/10.1109/59.331421>.
- Schniter P, Wozniak L. Efficiency based optimal control of kaplan hydrogenerators. *IEEE Trans Energy Convers* 1995;10(2):348–53. <https://doi.org/10.1109/60.391902>.
- Brezovec M, Kuzle I, Tomisa T. Nonlinear digital simulation model of hydroelectric power unit with kaplan turbine. *IEEE Trans Energy Convers* 2006;21(1):235–41. <https://doi.org/10.1109/TEC.2005.847963>.
- Yang W. *Hydropower plants and power systems: dynamic processes and control for stable and efficient operation [Ph.D. thesis]*. Uppsala University; 2017.
- Yang W, Norrlund P, Chung CY, Yang J, Lundin U. Eigen-analysis of hydraulic-mechanical-electrical coupling mechanism for small signal stability of hydropower plant. *Renew Energy* 2018;115:1014–25. <https://doi.org/10.1016/j.renene.2017.08.005>. URL: <http://www.sciencedirect.com/science/article/pii/S0960148117307577>.
- Souza OH, Barbieri N, Santos AHM. Study of hydraulic transients in hydropower plants through simulation of nonlinear model of penstock and hydraulic turbine model. *IEEE Trans Power Syst* 1999;14(4):1269–72. <https://doi.org/10.1109/59.801883>.
- Xu B, Chen D, Behrens P, Ye W, Guo P, Luo X. Modeling oscillation modal interaction in a hydroelectric generating system. *Energy Convers Manage* 2018;174:208–17. <https://doi.org/10.1016/j.enconman.2018.08.034>. URL: <http://www.sciencedirect.com/science/article/pii/S0196890418308835>.
- Zhang H, Chen D, Xu B, Wu C, Wang X. The slow-fast dynamical behaviors of a hydro-turbine governing system under periodic excitations. *Nonlinear Dyn* 2017;87(4):2519–28. <https://doi.org/10.1007/s11071-016-3208-0>.
- Mo W, Chen Y, Chen H, Liu Y, Zhang Y, Hou J, et al. Analysis and measures of ultralow-frequency oscillations in a large-scale hydropower transmission system. *IEEE J Emerg Sel Top Power Electron* 2018;6(3):1077–85. <https://doi.org/10.1109/JESTPE.2017.2759810>.
- Villegas Pico H, McCalley JD, Angel A, Leon R, Castrillon NJ. Analysis of very low frequency oscillations in hydro-dominant power systems using multi-unit modeling. *IEEE Trans Power Syst* 2012;27(4):1906–15. <https://doi.org/10.1109/TPWRS.2012.2187805>.
- Yang W, Norrlund P, Bladh J, Yang J, Lundin U. Hydraulic damping mechanism of low frequency oscillations in power systems: quantitative analysis using a nonlinear model of hydropower plants. *Appl Energy* 2018;212:1138–52. <https://doi.org/10.1016/j.apenergy.2018.01.002>. URL: <http://www.sciencedirect.com/science/article/pii/S0306261918300023>.
- Xie R, Kamwa I, Rimorov D, Moeini A. Fundamental study of common mode small-signal frequency oscillations in power systems. *Int J Electr Power Energy Syst* 2019;106:201–9. <https://doi.org/10.1016/j.ijepes.2018.09.042>. URL: <http://www.sciencedirect.com/science/article/pii/S0142061518319513>.
- Zhao Y, Liao W, Ji Q, Zhou S, Luo X. Internal flow research and fluid-solid coupling analysis for bulb turbine with considering gravity affect and non-uniform inflow. 17th international symposium on transport phenomena and dynamics of rotating machinery (ISROMAC 2017). 2017. p. 1–6.
- Kubota T, Tsukamoto T. Scale effect on cavitation characteristics of low head large bulb turbine. *Fuji Electr Rev* 1990;36(2):59–63.
- Jošt D. Cavitation prediction for water turbines. *Proc. of ACCUSIM summer school conference*, 2017. 2017. p. 17–8.
- Brezovec M. *Mathematical model of bulb hydropower unit for determining the cause of power oscillations [Ph.D. thesis]*. University of Zagreb, Faculty of Electrical Engineering and Computing; 2018.
- Brezovec M, Kuzle I, Krpan M, Holjevac N. Analysis and treatment of power oscillations in hydropower plant dubrava. *IET Renew Power Gener* 2020;14:80–9. URL <https://digital-library.theiet.org/content/journals/10.1049/iet-rpg.2019.0523>.
- Maljković Z, Gašparac I, Žarko D, Magić D. Oscillations in bulb type hydropower unit. *Producerea, transportul si distributia energiei electrice si termice* 2005;1:20–3.
- Bajić B. Turbine instability explained by multidimensional cavitation diagnosis. *Proc. of the international conference HYDRO 2003*. 2003. p. 1–5.
- Jurić V, Zrinski G, Brezovec M. Dubrava hpp tailwater drawdown due to downstream river erosion. *Proc. of the international conference HYDRO 2008*. 2008. p. 1–5.
- Brezovec M, Kuzle I, Krpan M. Detailed mathematical and simulation model of a synchronous generator. *J Energy* 2015;64(1–4):102–29.